Available online at www.sciencedirect.com

ScienceDirect

Procedia Structural Integrity 44 (2023) 1458–1465

Structural Integrity Procedia

www.elsevier.com/locate/procedia

XIX ANIDIS Conference, Seismic Engineering in Italy

3D numerical characterization of a dissipative connection system for retrofit of prefabricated existing RC sheds

C. Pettorruso[a]*, V. Quaglini[a], E. Bruschi[a], L. Mari[b]

[a]*Politecnico di Milano, Department of Architecture, Built environment and Construction engineering ABC*
[b]*DVS; l.mari@dvs.vision*

Abstract

Prefabricated industrial sheds featured a high seismic vulnerability during the 2012 Emilia earthquake (Italy). The buildings typically exhibited a rigid collapse mechanism that was a consequence of the loss of support between columns, beams and roof elements.

The study presents a numerical characterization of a novel dissipative connection system (DCS) designed to improve the seismic performance of industrial sheds. The device, which is placed on the top of the columns, exploits the movement of a rigid body on a sloped surface to provide horizontal stiffness and control the lateral displacement of the beam.

A 3D finite element model of the prototype is formulated in Abaqus and used to switch the backbone curve from the scaled model to the full-scale device. A parametric study is conducted to evaluate the influence of the slope of the contact surface and the coefficient of friction on the output force of the system.

In the second part of the study, non-linear dynamic analyses are performed on a finite element model of a portal frame implementing, at beam-column joints, either the DCS or a pure friction connection. The results highlight the effectiveness of the DCS in controlling beam-to-column displacements, reducing shear forces on the top of columns, and limiting residual displacements that can accrue during ground motion sequences.

Keywords: prefabricated sheds, energy dissipation, seismic retrofit, beam-to-column connection, recentering

* Corresponding author. Tel.: +390223995108
E-mail address: carlo.pettorruso@polimi.it

10.1016/j.prostr.2023.01.187

1. Introduction

Recent earthquakes have dramatically reaffirmed the seismic vulnerability of prefabricated industrial sheds typical of past Italian practice. The Emilia earthquake of May 2012 hit an area with a high density of productive activities, striking mainly industrial buildings in precast reinforced concrete (RC) [Belleri et al. (2015a), Bosio et al. (2020)] rather than in steel [Formisano et al. (2018)]. The structural deficiencies of this kind of structures are primarily related to the mechanisms of transmission of horizontal loads between structural elements [Belleri et al. (2015b)]; in fact, their static scheme consists of structural elements (beams, columns, and roof elements) connected with joints usually realized in simple support or through pin-end connections with insufficient resistance to seismic loads. This kind of connections relies solely on friction and is inadequate to properly transfer the horizontal loads [Belleri et al. (2014), Liberatore et al. (2013), Magliulo et al. (2008)] and accommodate compatible rotations and displacements [Brunesi et al. (2015), Casotto et al. (2015), Colombo et al. (2016)]. Indeed, the most common failures, causing the collapse of entire portions of buildings, included drop of roof elements and precast beams due to the loss of support, and collapse of the forks at the top of columns caused by off-axis loads.

Within the framework of global retrofit interventions, the study aims at introducing a novel dissipative connection system (DCS), designed to improve the behavior of beam-to-column connections and reduce the seismic vulnerability of precast RC industrial buildings [Mari et al. (2021)]. The DCS, which is placed on the top of columns, is basically composed of two mating truncated-pyramidal steel plates, one concave and the other one convex in shape and is intended to transmit vertical and horizontal loads at the node. The system exploits the movement of a rigid block sliding on a sloped surface to provide horizontal stiffness and a certain re-centering effect and dissipates part of seismic energy by friction.

In the present study, a 3D model of the DCS is firstly formulated based on experimental data [Quaglini et al. (2022), Mari et al. (2021)], and then the DCS is assessed under seismic loading by means of nonlinear analyses conducted on a portal frame of an industrial shed.

2. 3D characterization

2.1. Prototype and response

The study is conducted by referring to a DCS unit rated for a vertical load N_d = 360 kN and a horizontal deflection d_{bd} = 60 mm. In order to match the capacity of the available testing equipment, the experimental characterization was performed on a DCS prototype scaled by a geometric factor S_L = 0.4 and fabricated in steel, which resulted in a design vertical load of the prototype $N_{d,s}$ = 57.6 kN and a related design deflection $d_{bd,s}$ = 24 mm [Mari et al. (2021), Quaglini et al. (2022)]. The main dimensions of the DCS prototype are shown in Fig. 1.

The experiments were performed at the Materials Testing Laboratory of Politecnico di Milano, using a proprietary biaxial testing system [Quaglini et al. 2012].

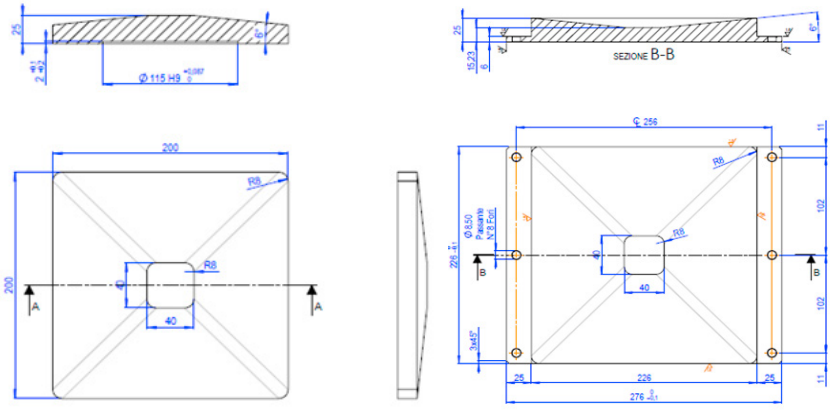

Fig. 1 – Geometry [in mm] of the small-scale prototype of the DCS: (a) convex plate; (b) concave plate [Quaglini et al. (2022)]

The prototypes exhibited an almost rigid-plastic behavior in X and Y direction, where it is possible to recognize four different phases, as shown in Fig. 2: (1) at the beginning of the motion, before sliding between the mating surfaces of the two plates is triggered, the force follows an almost proportional relationship with the displacement; (2) when sliding between the convex and the concave plate is engaged, a constant force is developed independently of the deflection; (3) when the convex plate reaches the boundary of the concave plate, and the actual contact area between the mating surfaces of the two plates decreases, the force too undergoes a decrease; (4) when the convex plate moves back to the origin, the reaction force is virtually negligible.

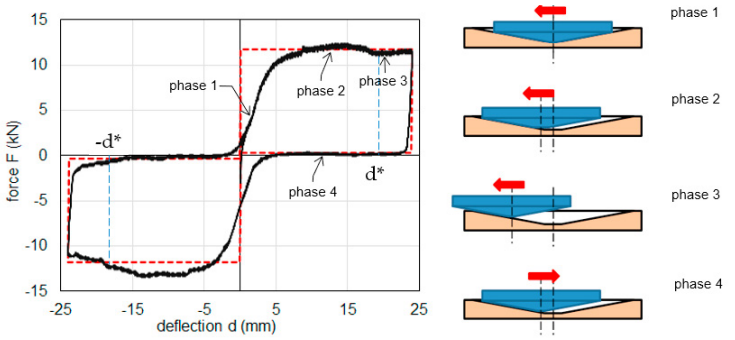

Fig. 2 – **Constitutive behavior of the DCS and different phases of motion [Quaglini et al. (2022)]**

2.2. Numerical description

Numerical model of the DCS described above was developed using the Abaqus CAE finite element calculation program and its references. The geometry of the numerical model replicated the dimensions of the prototype subjected to experimental characterization tests at the Politecnico di Milano.

The numerical model included only the two plates, disregarding the connections (Fig. 3).

Numerical analyses were performed by subjecting the FEM model, to a biaxial load. The boundary conditions that characterize the convex element are the distributed pressure of 11 MPa, whose resultant is 57,6 kN, applied on the external face, and the harmonic displacement with amplitude 24 mm. The concave element is fixed.

The numerical model was divided into a mesh of finite elements type C3D8 (three-dimensional hexahedral element with 8 nodes) with maximum dimension equal to 8 mm. A total of #1016 elements were used for the convex element and #2034 elements for the concave element (Fig. 3). The contact between the surfaces was modeled through the surface-to-surface contact command, defining the convex element as the master element, and formulating a hard contact constitutive behavior in the direction perpendicular to the contact surface, and a penalty constitutive behavior tangentially the contact surface [Quaglini et al. (2019)] with coefficient of friction $\mu = 0.11$, as determined from the experiments on DCS. The additional information on element properties is reported in Mari et al. (2021). An implicit dynamic analysis with full Newton solution technique was carried out.

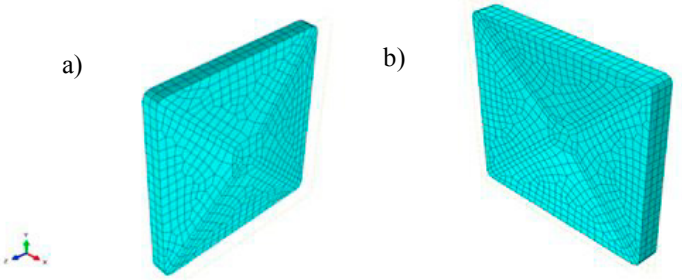

Fig. 3 – FEM model of the DCS:(a) convex element; (b) concave element

The results of the numerical analyses are shown below for two trajectories of motion of the convex component with respect to the concave component defined by angle θ (Fig. 4).

The DCS is analyzed according to the angles $\theta = 0°$ and $\theta = +90°$; the results are expressed in the form of force-displacement curves and reaction moment-displacement curves (Fig. 5).

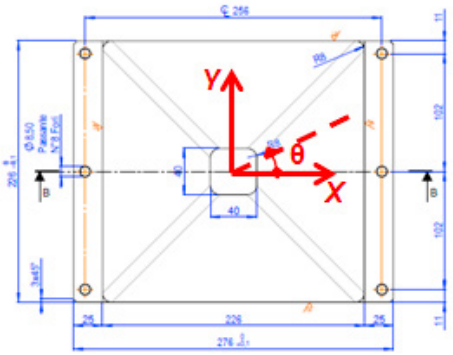

Fig. 4 – Definition of the reference system for the displacements

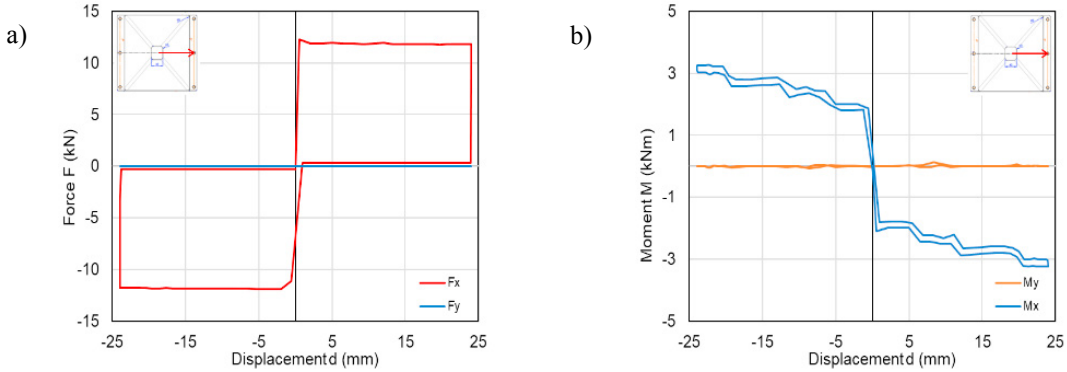

Fig. 5 – (a) Force-displacement and (b) Moment-displacement at top of column

The component of the reaction force developed in the direction of motion is almost constant and the component along the perpendicular direction is zero (Fig. 5a), and this is justified by the symmetry of the contact surfaces with respect to the direction of motion.

The reaction bending moment evaluated at the top of the column (Fig. 5b), in agreement with the reaction, acts only in the plane parallel to the direction of displacement, while in the perpendicular plane is zero. The moment can be split in two contributions, the first due to the horizontal reaction force F and the second due to the eccentricity of the vertical force N due to the displacement of the convex element.

Eventually, Fig. 6 compares the force-displacement curves obtained from the numerical analyses and the experimental curves from the tests conducted at Politecnico di Milano.

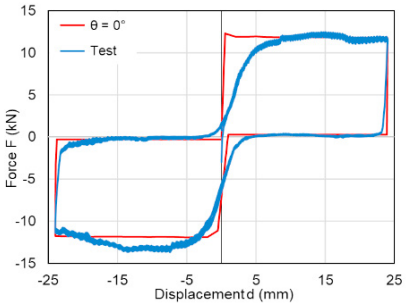

Fig. 6 – Comparison between experimental and numerical force-displacement curves

The correspondence between the experimental curves and the results of the numerical analyses is very fair. The biggest deviations occurring close to the origin of the displacement axis and are attributed to the effect of the inertial forces at the onset of the motion, not reproduced in the numerical analyses.

3. Numerical Investigation - Case study

To assess the performance of the DCS and evaluate its effectiveness in comparison to the pure friction beam-to-column joints typical of past building practices, non-linear dynamic analyses of a prefabricated shed structure were performed.

The model consists of a two-dimensional portal frame comprising two 50×60 cm columns and a 50×80 cm beam, with geometry and overall dimensions as shown in Figure 7. It was implicitly assumed that no secondary beams were placed orthogonally to the frame in order to ensure a 3D response of the structure. The columns are made of C40/50 concrete, reinforced longitudinally with 16 Ø20 steel bars (B450C class [Italian Building Code]) and transversally with Ø8 two-arm stirrups at 10 cm spacing. The distributed load acting on the beam, including its weight and the load from the contributory area of the roof, is 26.9 kN/m, resulting in a total seismic mass of 146.84 ton evaluated according to the Italian Building Code, and in a vertical force at either support of 360 kN, matching the design load of the DCS units.

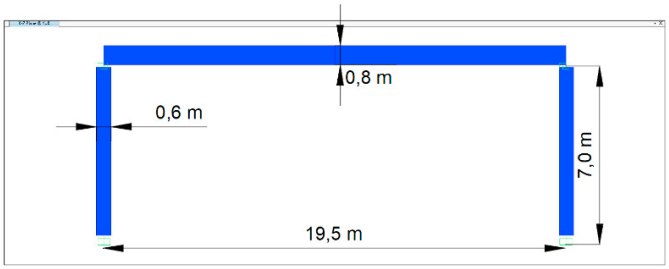

Fig. 7 – Portal frame model

The structural model was implemented in Sap2000 v21.1.0 software. The two columns were rigidly fixed to the ground and modelled as linear elastic elements, with a plastic (rotational) hinge at the basis formulated according to Table 10-8 (concrete columns) of ASCE 41-13 in order to account for anelastic concrete deformation. The beam was assumed to behave as a linear elastic body, and a "body" constraint [SAP2000 Analysis Reference] was introduced to enforce that the displacements at either end of the beam are identical.

For the beam-to-column pure friction connection, a constant friction coefficient $\mu_{cc} = 0.30$ was assigned, coupled to an isotropic hysteresis type (it must be noted that, to be conservative, one half of the concrete-to-concrete friction coefficient recommended in Eurocode 8 for smooth surfaces was adopted).

The fundamental period of the frame is T = 0.838 s. The internal structural damping is modeled as Raileigh damping, with parameters assigned to achieve 5% damping ratio at $T_1 = 0.838$ s and $T_2 = 0.611$ s.

Non-linear dynamic analyses were performed assuming a functional class II with nominal life 50 years, located in Potenza, South Italy, topographic category T1, soil type B. The target elastic spectrum was determined according to the Italian Building Code provisions for Life Safety Limit State (SLV). A set of seven unidirectional ground motions consistent with the target spectrum was selected with REXEL v3.4 beta [Iervolino, I. et al. (2010)] software from the European Strong-motion Database [Ambraseys, N. et al]. The magnitude (M_w) of the seven ground motions was chosen within the interval (6.4 – 7), with epicentral distance (Rep) in the range 0-30 km. The waveforms were scaled to the design Peak Ground Acceleration of 2.375 m/s^2 calculated according to the Italian Building Code. Relevant information on the ground motion data set is reported in Table 1. To be conservative, a vertical acceleration of 0.4 g was assumed, in order to reduce the resisting force of the connections and engage sliding at the beam-to-column interface either with the DCS or the pure friction joint.

Table 1. Accelerograms dataset.

Record	Waveform	EQ	Mw(-)	Rep(-)	PGA(m/s2)	PGV(m/s)	SF
South Iceland	6263ya	1635	6.5	7	5.018	0.4975	0.47338
South Iceland (aftershock)	6328ya	2142	6.4	12	3.8393	0.2005	0.61871
South Iceland	4673xa	1635	6.5	15	2.0382	0.122	1.1654
Montenegro	196ya	93	6.9	25	2.9996	0.253	0.79191
Campano Lucano	291ya	146	6.9	16	1.7247	0.2745	1.3773
Montenegro	199	93	6.9	16	3.5573	0.5202	0.66776
Campano Lucano	291xa	146	6.9	16	1.5256	0.271	1.557

	6.71	15.3	2.9575	0.3055	0.95022

Mw: magnitude; **Rep:** epicentral distance; **PGA:** Peak Ground Acceleration; **PGV:** peak Ground Velocity; **SF:** Scale Factor.

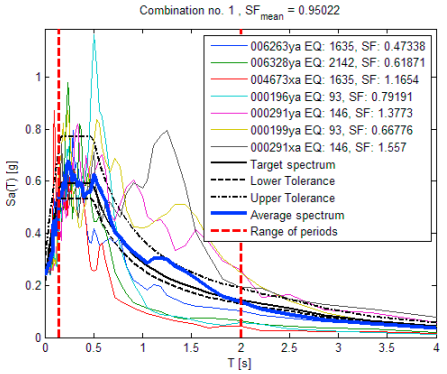

Fig. 8 – Scaled ground motion acceleration spectra and target spectrum according to the Italian Building Code (ξ = 5%).

The effectiveness of the DCS over the pure friction (P-F) joint has been examined in terms of (i) maximum resisting force of the beam-to-column joint F_{max}, (ii) maximum horizontal displacement of the beam with respect to the column d_{max}, and (iii) residual displacement of the beam at the end of the ground motion d_{res}. Fig. 9 shows the comparison of the seismic response of the DCS and P-F joints in terms of maximum force, maximum displacement and residual displacement of the seven accelerograms, while Fig. 10 shows the mean of the maxima of the response parameters over the set of seven accelerograms.

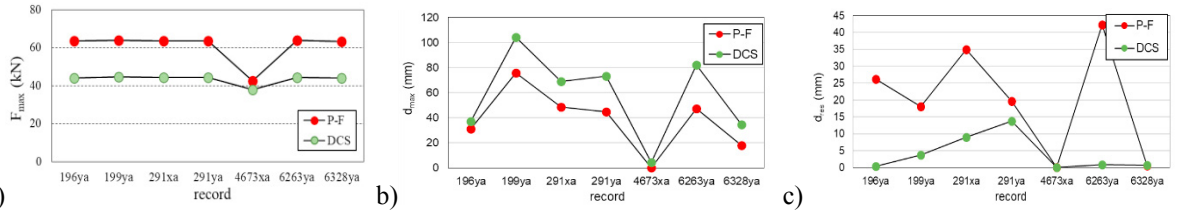

Fig. 9 – Comparison of the seismic response of DCS and pure friction (P-F) joints in terms of maximum force (a) a maximum displacement (b) and residual displacement for the set of 7 accelerograms

The P-F joint develops a maximum resisting force Fmax about 40% greater than the DCS; however, it better limits the displacement of the beam during the earthquake, with a maximum slippage of 38 mm vs. 58 mm of the DCS (Fig. 10). Nevertheless, it must be noted that the maximum displacement of the beam supported by the DCS, i.e., d_{max} = 57.8 mm, matches the design value d_{bd} = 60 mm of the system, and can therefore be accommodated by the mechanical joint. The most interesting result is the comparison in terms of the residual displacement: with the DCS the offset of the beam at the end of the ground motion is as small as d_{res} = 4 mm, whereas with the P-F joint the residual displacement is about 20 mm.

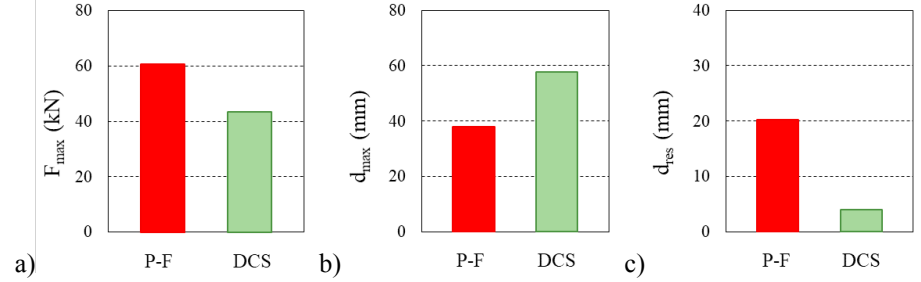

Fig. 10 – Comparison of the seismic response of DCS and (P-F) joint in terms of: (a) maximum force; (b) maximum displacement; (c) residual displacement [Quaglini et al. (2022)]

Analyzing the hysteretic loops of the two joints for accelerogram 291xa, Fig. 11, it is possible to notice both the elastoplastic behavior of the DCS, with the expected recentering behavior as the driving force changes its direction, and the unbalanced behavior, in terms of displacements, in the P-F case. In particular it is evident in the response of the PF-system the occurrence of a permanent deformation which is not recovered but increases each time the driving force is enough to trigger sliding of the surfaces. This is reflected in the relevant displacement histories (Fig. 11c), and it is interesting to note the accrual of permanent deformation affecting the response of the P-F joint, whereas the residual displacement of the DCS at the end of the ground motion is negligible.

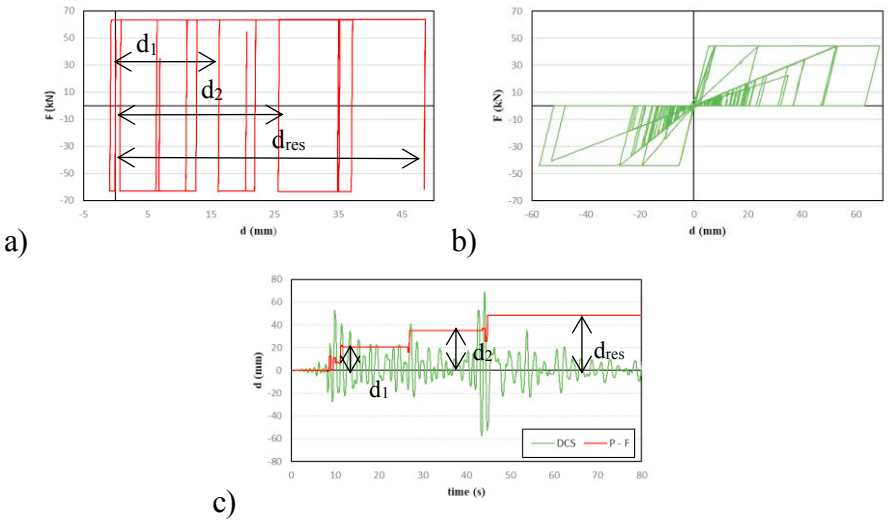

Fig. 11 - Response of the connection systems to accelerogram 291xa: (a) hysteretic loop of P - F joint; (b) hysteretic loop of DCS joint; (c) displacement histories

This is due to the fact that the sliding motion of the P-F joint is engaged when the seismic action exceeds the friction resistance at the beam-to-column interface, and therefore occurs only during the strong motion stage of the earthquake. During the coda stage the ground acceleration is not sufficient to trigger sliding, and the beam remains in the offset position achieved at the end of the previous stage, leading to a huge residual displacement. In contrast, the DCS develops larger displacements during the strong motion stage (Fig. 11b) but owing to the restoring force provided by the sloped surfaces, it tends naturally to recover the original configuration as the ground acceleration gets down.

4. Conclusions

In the present work a dissipative connection system (DCS), intended for the seismic protection of precast RC industrial sheds, has been investigated in an experimental campaign and by formulating a 3D numerical model and performing non-linear dynamic analyses to prove the effectiveness of this system over the traditional pure friction joints.

The force-displacement curves obtained from the 3D numerical analyses carried out on the prototype and the corresponding experimental curves show an acceptable correspondence.

Non-linear dynamic analyses proved the effectiveness of the DCS to control the relative displacements at the beam-to-column joint, and the maximum shear force transmitted to the column head, and most importantly, the restoring capacity of the system, which is able to control the residual displacement at the end of the ground motion within small values. This feature is really important to guarantee the capability of the structure to withstand aftershocks, which can occur within a short time from the main shock, as occurred for example in the Centro Italia Earthquake 2016.

Acknowledgements

The authors wish to thank Mr. Roberto Minerva and the Materials Testing Laboratory of the Politecnico di

Milano for making the experimental equipment available and Mr. Giacomo Vazzana for assistance during the execution of the tests.

References

Abaqus/CAE 2017 Documentation. Analysis User's Manual, Simulia; 2017.

Ambraseys N, Smit P, Sigbjornsson R, Suhadolc P, Margaris B. Internet-Site for European Strong-Motion Data, European Commission, Research-Directorate General, Environment and Climate Programme. Available online: http://www.isesd.cv.ic.ac.uk/ESD/ (accessed on 24 November 2021).

ASCE/SEI 41-13 Seismic Evaluation and Retrofit of Existing Buildings; American Society of Civil Engineers: Reston, VA, USA, 2014.

Belleri A, Moaveni B, Restrepo JI (2014) Damage assessment through structural identification of a three-story large-scale precast concrete structure, Earthquake Engineering & Structural Dynamics, 43(1), p. 61-76.

Belleri A, Torquati M, Riva P, Nascimbene R (2015a) Vulnerability assessment and retrofit solutions of precast industrial structures, Earthquakes and Structures, Vol. 8 No. 3, p. 801-820.

Belleri A, Brunesi E, Nascimbene R, Pagani M, Riva P (2015b) Seismic performance of precast industrial facilities following major earthquakes in the Italian territory. Journal of Performance of Constructed Facilities, 29, 04014135, DOI: 10.1061/(ASCE)CF.1943-5509.0000617.

Bosio M, Belleri A, Riva P, Marini A (2020) Displacement-based simplified seismic loss assessment of Italian precast buildings, Journal of Earthquake Engineering, Vol. 24, No. S1, p. 60-81.

Brunesi E, Nascimbene R, Bolognini D, Bellotti D (2015) Experimental investigation of the cyclic response of reinforced precast concrete framed structures, PCI Journal15 (2), p. 57–79, DOI: 10.15554/pcij.03012015.57.79.

Casotto C, Silva V, Crowley H, Nascimbene R, Pinho R (2015) Seismic fragility of Italian RC precast industrial structures, Engineering Structures 94, p. 122–136, DOI: 10.1016/j.engstruct.2015.02.034.

Colombo A, Negro P, Toniolo G, Lamperti M (2016) Design guidelines for precast structures with cladding panels, JRC Technical report, ISBN 978-92-79-58534-0.

Italian Building Code - CSLLPP (Consiglio Superiore dei Lavori Pubblici). D.M. 17 gennaio 2018 in materia di "norme tecniche per le costruzioni". Gazzetta ufficiale n.42 del 20 febbraio 2018, Supplemento ordinario n.8, Ministero delle Infrastrutture e dei trasporti, Roma; 2018, in Italian.

Formisano A, Di Lorenzo G, Landolfo R (2018) Seismic retrofitting of industrial steel buildings hit by the 2012 Emilia-Romagna earthquake: a case study, Conference Proceedings – October 2018.

Liberatore L, Sorrentino L, Liberatore D, Decanini LD (2013) Failure of industrial structures induced by the Emilia (Italy) 2012 earthquakes, Engineering Failure Analysis, 34, p. 629-647.

Iervolino I, Galasso C, Cosenza E (2010) REXEL: Computer aided record selection for code-based seismic structural analysis. Bulletin of Earthquake Engineering, 8, p. 339–362, DOI: 10.1007/s10518-009-9146-1.

Magliulo G, Fabbrocino G, Manfredi G (2008) Seismic assessment of existing precast industrial buildings using static and dynamic nonlinear analyses", Eng. Struct., 30(9), 2580-2588.

Mari L, Quaglini V, Pettorruso C, Bruschi, E (2021) Experimental and numerical assessment of isolation seismic device for retrofit of industrial shed, In Proceedings of the COMPDYN 2021 and 8th ECCOMAS Thematic Conference on Computational Methods in Structural Dynamics and Earthquake Engineering, Athens, Greece, 27–30 June 2021; Papadrakakis, M.; Fragiadakis, M. (Eds.), p. 3187.

Quaglini V, Dubini P, Poggi C (2012) Experimental assessment of sliding materials for seismic isolation systems, Bulletin of Earthquake Engineering, 10, 717-740, DOI: 10.1007/s10518-011-9308-9.

Quaglini V, Gandelli E, Dubini P (2019) Numerical investigation of curved surfaced sliders under bidirectional orbits, Ingegneria Sismica - International Journal of Earthquake Engineering, Vol. 2.

Quaglini V, Pettorruso C, Bruschi, E, Mari L (2022) Experimental and numerical investigation of a dissipative connection for the seismic retrofit of precast RC industrial sheds. Geosciences 2022, 12, 25. https://doi.org/10.3390/geosciences12010025.

SAP2000 Analysis Reference, Volume 1; Computer and Structures Inc.: Berkeley, CA, USA, 1997.